Cluster and Periodic Calculations of the Ethene Protonation Reaction Catalyzed by theta-1 Zeolite: Influence of Method, Model Size, and Structural Constraints

Mercè Boronat,[a] Claudio M. Zicovich-Wilson,[a] Pedro Viruela,[b] and Avelino Corma*[a]

Abstract: The protonation of ethene by three different acid sites of theta-1 zeolite was theoretically studied to analyze the extent and relevance of the following aspects of heterogeneous catalysis: the local geometry of the Brønsted acid site in a particular zeolite, the size of the cluster used to model the catalyst, the degree of geometry relaxation around the active site, and the effects related to medium- and long-range interactions between the reaction site and its environment. It has been found that while the reaction energy is very sensitive to the local geometry of the site, the activation energy is mainly affected by the methodology used and by electrostatic effects on account of the carbocationic nature of the transition state.

Keywords: ab initio calculations · cluster models · density functional calculations · heterogeneous catalysis · zeolites

Introduction

Acidic zeolites play an important role in the petroleum and chemical industries as solid catalysts for a number of hydrocarbon reactions, such as isomerization, oligomerization, alkylation, and cracking.[1, 2] For a long time it has been accepted that the mechanism of heterogeneous catalysis over solid acids is analogous to that of homogeneous reactions in the gas phase or superacid media, and that carbenium and carbonium ions are the intermediate species formed by the interaction of hydrocarbon molecules with the Brønsted acid sites in the zeolite.[3, 4] However, the carbocation-based mechanisms developed for zeolites are too simple, since they do not take explicit consideration of the solid and consequently they can not provide information about the exact nature of the reaction-activated complexes and intermediates, or the catalytic role played by the zeolite.

In this sense, quantum chemistry is a powerful tool to obtain a clearer insight into these reaction mechanisms. It allows the analysis of some aspects of heterogeneous catalysis that can not be directly studied by means of experimental techniques, such as the structure and nature of the reaction intermediates and transition states through which the processes occur, or the activation energies involved in the different elemental steps of the reaction. The main problem that arises when studying the mechanism of solid-acid catalyzed reactions by quantum chemistry is the very large dimensions of the catalyst particle that makes the rigorous treatment of the solid difficult. For this reason, the systems are generally simplified following several approaches. In this way, in the cluster model, a part of the solid catalyst (usually the active site) is simulated by a limited number of atoms that are "extracted" from the system and treated as a molecule. This approach allows the use of high-quality theoretical methods and the optimization of minima and transition-state geometries as well as frequency calculations. It is, therefore, particularly suited to describe local phenomena, such as the interaction of organic molecules with catalytically active sites. It has been successfully applied to investigate the interaction of methanol[5, 6] with Brønsted acid sites, the protonation of olefins,[7] the adsorption of carbenium ions,[8] the H/D exchange between alkanes and the zeolite acid sites,[9–11] the dehydrogenation[10, 11] and cracking[11–14] of alkanes, the isomerization of hydrocarbons,[15, 16] the hydride transfer between alkanes and alkenes,[17, 18] the paraffin/olefin alkylation,[19] etc.

One of the disadvantages of the cluster approach is that the systems often used to model the active site in the zeolite $(HO(H)Al(OH)_3$, SiX_3-OH-AlX_3, or SiX_3-OH-AlX_2-$OSiX_3$, with X = H, OH) are not typical of any particular zeolite and therefore they are not able to explain the different catalytic behavior exhibited by structurally different zeolites. Other limitations of this approach are derived from neglecting the long-range electrostatic effects caused by the Madelung

[a] Prof. Dr. A. Corma, Dr. M. Boronat, Dr. C. M. Zicovich-Wilson
Instituto de Tecnología Química UPV-CSIC Universidad Politécnica de Valencia
Av/ dels Tarongers, s/n, 46022 Valencia (Spain)
Fax: (+34) 96-387-7809
E-mail: acorma@itq.upv.es

[b] Prof. Dr. P. Viruela
Departament de Química Física, Universitat de València
C/ Dr. Moliner 50, 46100 Burjassot (Spain)

  0947-6539/01/0706-1295 $ 17.50+.50/0

potential of the crystal and the appearance of border effects where the cluster is separated from the rest of the solid.

In the periodic approach, the host catalyst is represented by an infinite perfect crystalline system. The calculations take advantage of the translational symmetry of the crystal and therefore the long-range electrostatic effects are included in a very natural way, while boundary effects are absent. In particular, the implementation of theory based on Gaussian-type atomic orbitals (GTAO)[20] is a useful tool to be used in quantum-chemical research because it can provide accurate information on the physicochemical properties of solid state-materials at the same methodological level (basis sets, Hamiltonians) as available in standard quantum-chemistry codes. This approach has been recently employed in several studies on the catalytic properties of zeolites[21, 22] with quite satisfactory performance. Unfortunately, at present, the evaluation of analytic derivatives of the energy with respect to the structural parameters is not yet implemented in periodic codes that use GTAO. Geometry optimizations of large systems is, in general, a hard task and limits the suitability of this approach in reactivity studies.

The aim of this work is to evaluate the extent and relevance of the following aspects of heterogeneous catalysis: a) the local geometry of the active site in a particular position of a particular zeolite, b) the size of the cluster used to model the catalyst and the degree of geometry relaxation around the active site, as well as c) the effects related to medium- and long-range interactions between the reaction site and its environment. The reaction chosen is the protonation of an olefin, ethene, by a zeolite Brønsted acid site. This process was first studied by Kazansky et al.[23] with the $[HO(H)Al(OH)_3]$ cluster at the HF/3-21G theoretical level. They found that protonation of ethene results in the formation of a stable and covalently bound surface ethoxide, and that the reaction proceeds through a transition state in which the geometry and electronic structure of the organic fragment resembles that of a carbenium ion. The same results were later obtained for propene, *n*-butene, and isobutene by the use of larger clusters and calculations methods at a higher level of theory.[7, 15] In all cases it was found that the reaction intermediates formed are not ionic but covalent alkoxides, and that these alkoxides are several kcal mol^{-1} more stable than the adsorbed olefins. In agreement with these results, a number of ^{13}C NMR MAS spectroscopic studies have detected alkyl groups covalently bound to the framework oxygen atoms on the surface of acidic zeolites.[24–27]

All these theoretical studies were performed within the cluster approach, with its previously mentioned limitations, and with small models that do not represent any existing/real zeolite. In contrast, we have now investigated the ethene protonation reaction with models that represent different active sites of a particular zeolite, and theoretical methods that include most effects of relevance in heterogeneous catalysis. The geometries of the ethene molecule adsorbed on the Brønsted acid site, of the resulting covalent ethoxide, and of the transition state for the process have been optimized with the cluster approach and both Hartree – Fock and density functional theory (DFT) calculations. Apart from a general $H_3Si\text{-}OH\text{-}AlH_2\text{-}O\text{-}SiH_3$ cluster, four different acid sites of zeolite theta-1 have been considered, as explained in the next section. The influence of the framework flexibility has been analyzed by optimization of the geometry of the three species involved adsorbed on clusters of increasing size. Finally, the long-range effects have been evaluated by periodic calculations on the optimized structures. It has been found that when the geometry of the active site is somehow restricted to represent a particular position in the framework, the structural changes necessary to accommodate the ethoxide complex become more difficult and, as a consequence, the ethoxide is destabilized in relation to the ethene π complex. The same trend was reported in a previous study of alkene chemisorption in chabazite,[28] although the alkoxide destabilization in that case was not as important as that found in the present work. It has also been observed, in agreement with previous work,[28–30] that because of the ionic character of the transition state, the activation energies are greatly influenced by electrostatic effects, especially those of short and medium range.

Models and Methods

Theta-1 is a unidimensional medium-pore high-silica zeolite that exhibits valuable properties, such as thermal stability, shape-selectivity, and acidic character. The silicon framework of theta-1 is composed of 5-T and 6-T rings (where 5-T ring is a ring containing five tetrahedrally coordinated centers) which link to form 10-T-ring channels parallel to *c* (Figure 1). There are four crystallographically distinct T atoms of relative occupancy 4:4:8:8. The refined orthorhombic $Cmc2_1$ structure of pure silica theta-1[31, 32] was used as a starting point. The unit cell was duplicated in the channel direction and one Al and one H atom were introduced to create a Brønsted acid site. The primitive cell of the H-zeolite obtained contains 73 atoms and a Si/Al ratio of 23. The geometry of the system was then optimized with molecular mechanics techniques with GULP[33] and the shell-model force field derived by Schröder and Sauer.[34] The Al atom was introduced into the T1, T2, and T3 positions, and the proton was placed only on those oxygen atoms linked to the corresponding Al center that resulted in a bridging hydroxy group pointing towards the 10-T ring. By the exclusion of T4 and the H atoms pointing towards the 5-T or the 6-T rings, we made sure that all the active sites studied are accessible to organic molecules.

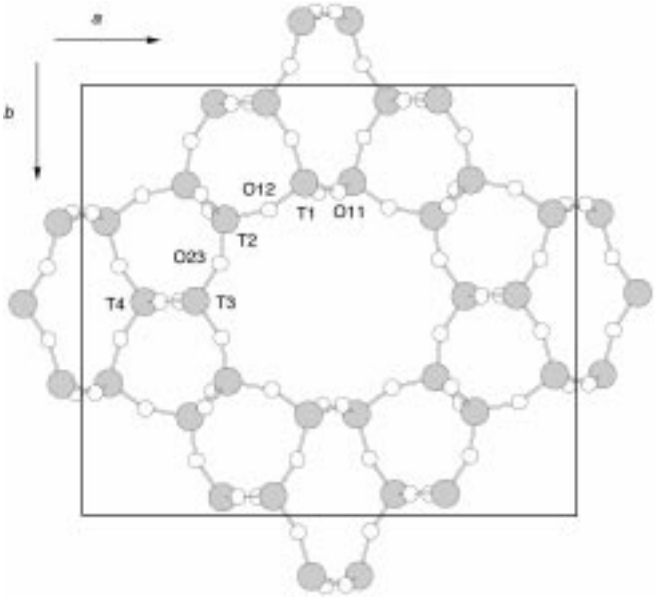

Figure 1. Structure of theta-1 framework showing the atom-labeling scheme.

0947-6539/01/0706-1296 $ 17.50+.50/0 *Chem. Eur. J.* **2001**, *7*, No. 6

Three clusters of different size were then cut out from each one of the resulting structures (Figure 2). Cluster **B** contains the central aluminum atom, the four oxygen atoms bonded to it, the four silicon atoms bonded to the oxygens and the hydrogen atom which forms the bridging hydroxy group. In cluster **C**, two coordination spheres were added to the two silicon atoms bonded to the oxygen atoms involved in the ethene protonation reaction. Cluster **D** includes two complete 10-T rings of the unidimensional channel and all the atoms of cluster **C**. In all cases, the dangling bonds that connect the cluster to the rest of the solid were saturated with hydrogen atoms at 1.49 Å from the silicon atoms and orientated towards the positions occupied in the crystal by the oxygen atoms in the next coordination sphere. For the sake of comparison, the previously used H_3Si-OH-AlH_2-$OSiH_3$ model (cluster **A** in Figure 2) was also included in the study.

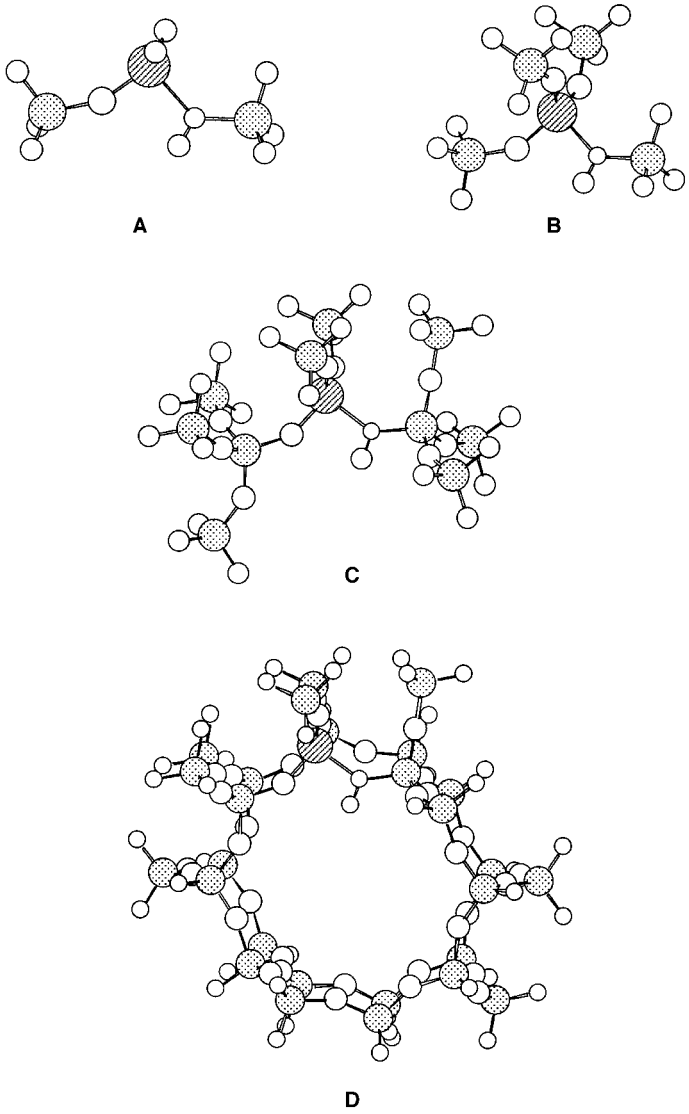

Figure 2. Cluster models used in this work.

The geometries of the π complex formed by adsorption of ethene onto the active site, of the covalent ethoxide, and of the transition state for the process were optimized with clusters **A**, **B**, and **C** to simulate the solid catalyst. When cluster **A** was used, all geometric parameters were fully optimized except the dihedral angles of the silicon atoms, in order to keep the heavy atoms of the cluster in the same plane. When clusters **B** and **C** were used, the terminal SiH_3 groups were kept fixed at their original positions and the coordinates of all other atoms were completely optimized. These calculations were performed both at the Hartree–Fock and density functional B3LYP[35] levels using the standard 6-31G* basis set[36] and the Berny analytical gradient method[37] as implemented in the Gaussian 94 computer program.[38]

Then, the optimized structures obtained with cluster **C** were introduced into cluster **D**, which contains two complete 10-T rings of the theta-1 unidimensional channel, and single-point calculations of the energy of the resulting systems were carried out. The basis set employed is a standard 6-31G** for the hydrogen, oxygen, and carbon atoms, while 6–21G* was used for the silicon atoms. The exponents of the most diffuse Gaussians in the cases of Si and O have been reoptimized for periodic calculations.[39] For the aluminum atoms, a nonstandard 8/511/1 (s/sp/d) set was used. For the sake of comparison, single-point calculations with this basis set were performed for the structures previously optimized using clusters **A**, **B**, and **C**.

Finally, to test the influence of the long-range effects neglected in the cluster approach, the HF/6-31G* optimized structures obtained with cluster **C** were reinserted into the original periodic framework and single-point energy calculations were performed at the HF theoretical level with the CRYSTAL98 software package[40] and the previously mentioned basis set. The standard tolerances proposed in the manual were used for the integral evaluation, and eight *k* points (shrinking factor 2) were used for sampling within the Brillouin Zone.

Results and Discussion

Active sites: Table 1 summarizes the relative stability of the five Brønsted sites in theta-1 that are accessible to organic molecules. The results of the molecular mechanics optimizations indicate that all sites are equally stable, except the T1 site with the proton located on O12, and therefore this site has not been henceforth considered. The most stable conformation at this level of theory was obtained for the Al atom situated at T2, no matter whether the proton was located on O12 or on O23, the T1/O11 and T3/O23 sites were slightly less stable. The geometry of these sites was reoptimized with the cluster **C** model and the HF/6-31G* method; it was found that the most stable conformation at this level corresponds to the Al atom situated in the T2 position with the proton located on O12. Since the present study of the ethene protonation reaction is mainly based on the cluster approach, we have considered that when the Al atom is in the T2 position (from now on T2 site) the initial reactant will be ethene adsorbed on the proton located on O12 and the ethoxide will be formed on O23. When the Al atom is situated at T1, the most stable conformation corresponds to the proton located on O11, but the ethoxide can be formed either on O12 or on the other O11 atom bonded to T1. The two possibilities have been considered and, therefore, there are two different cluster models associated with this site, T1a and T1b, respectively. Finally, in the case of the Al atom situated at T3, both the proton of the

Table 1. Relative energies [kcal mol^{-1}] of the theta-1 Brønsted acid sites considered in this work.

Al–O	MM	cluster **C** (HF)	Periodic (HF)
T1–O11	0.93	3.58, 3.74	2.99, 3.00
T1–O12	2.33		
T2–O12	0.14	0.00	0.00
T2–O23	0.00	0.69	
T3–O23	0.92	0.77	0.92

Brønsted acid site and the ethoxide are located on O23, and therefore there is only one cluster model named T3.

Table 2 summarizes the HF/6-31G*-optimized values of the most important geometric parameters of the **C** clusters corresponding to T1a, T1b, T2, and T3 acid sites. It can be seen that the geometry of the bridging hydroxy group is completely equivalent in all sites. Only in the case of the T1b cluster there are observable differences, such as the slightly shorter O2–Al bond length, the smaller Si-O2-Al angle, or the wider O1-Al-O2 angle. This is so because in the T1b cluster the O2 atom does not belong to the 10-T ring, but links two of these rings. Since the proton of the acid site always points towards the center of the 10-T ring, the calculated H-O1-Al-O2 dihedral angle value for T1b, -117.2°, is also completely different from the values obtained for the other sites, which are close to 0°.

Table 2. HF/6-31G*-optimized values of the most important geometric parameters of the four acid sites considered in this work obtained with cluster **C** (bond lengths in Å and angles in degrees). Net atomic charge (qH^+ in $|e|$), electrostatic potential (V_0 in V), and absolute value of the largest component of the traceless electric field gradient tensor (Q_H in $V Å^{-2}$) on the proton of the bridging hydroxy calculated at the periodic HF level. The atom numbering is shown in Figure 3.

	T1a	T1b	T2	T3
O1–H	0.955	0.955	0.956	0.955
O1–Si	1.681	1.682	1.685	1.689
O1–Al	1.905	1.907	1.913	1.905
H-O1-Al	105.7	104.9	106.0	109.2
Si-O1-Al	138.2	138.9	136.7	136.0
O1-Al-O2	91.4	101.6	92.0	95.8
O2–Si	1.593	1.592	1.594	1.593
O2–Al	1.721	1.709	1.718	1.712
Si-O2-Al	149.5	141.9	147.2	149.0
H-O1-Al-O2	9.4	−117.2	0.9	−6.5
qH^+	0.399	0.399	0.402	0.403
V_0	−31.926	−31.926	−31.919	−31.902
Q_H	23.880	23.880	23.818	24.001

It can also be seen in Table 2 that some electrostatic properties of the acid site, such as the positive charge or the largest component of the traceless electric field gradient tensor (Q_H) on the proton of the bridging hydroxy group, do not differ from one site to another. It has been shown that there is a linear relationship between Q_H and the vibrational frequency of the OH bond,[22] which is a measure of the acidity. The electric field on the proton was also calculated within the periodic approach, although it is known that for a system described by the exact electronic wavefunction the electric field at each nucleus is exactly zero for an equilibrium structure. In this case, the obtained values are ≈ 0.007 hartree $bohr^{-1} e^{-1}$ for two reasons: the basis set used in the calculations is not saturated and the geometry of the system has not been optimized within the periodic approach.[22] According to the calculated values, the intrinsic acidity of the four sites considered is similar. However, as discussed in the next sections, the activation and reaction energies calculated for the different sites are not equivalent. This indicates that it is not always possible to find a direct relationship between the intrinsic properties of the bridging hydroxy group and the activity of the site for a given reaction.

Geometry of the reaction species: The structures corresponding to ethene adsorbed on the Brønsted acid site, to the transition state for the studied reaction, and to the ethoxide complex obtained with cluster **B** are depicted in Figure 3; and Table 3 summarizes the HF- and B3LYP-optimized values of the most important parameters of these three systems calculated with clusters **A**, **B**, and **C**.

The optimized geometry of the π complex formed between ethene and the Brønsted acid site is quite independent of the method and the model used in the calculations. The C–C bond in ethene is 1.32 and 1.34 Å at the HF and B3LYP levels, respectively; the calculated O–H bond length is 0.96 Å at the HF level and 0.99 Å at the B3LYP level; and the C–H bond length obtained with the HF method, ≈ 2.5 Å, is slightly longer than that provided by the B3LYP functional, namely ≈ 2.3 Å. The most important difference between the HF- and DFT-optimized values corresponds to the Si-O2-Al angle: when clusters **B** or **C** are used, the values of the angle calculated with B3LYP are between $1-5^\circ$ smaller than the HF values; however, in the case of cluster **A** this difference

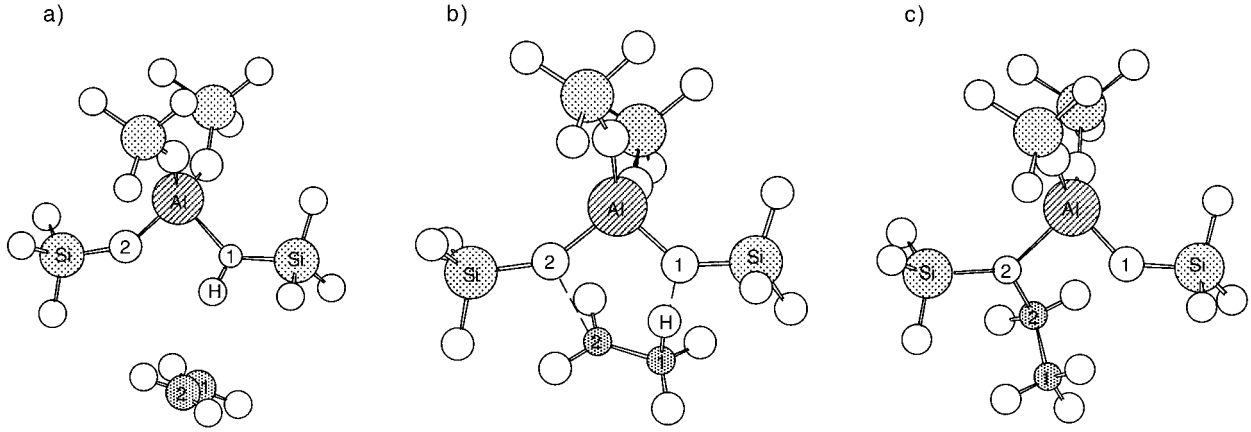

Figure 3. Optimized structures of a) ethene adsorbed on a Brønsted acid site, b) transition state for the ethene protonation reaction, and c) the ethoxide complex.

0947-6539/01/0706-1298 $ 17.50+.50/0 *Chem. Eur. J.* **2001**, *7*, No. 6

Table 3. HF/6-31G* and B3LYP/6-31G* (italics) optimized values of the most important geometric parameters of ethene, ethoxide and the transition state for the studied reaction (bond lengths in Å and angles in degrees). The atom numbering is shown in Figure 3.

site	T1a			T1b		T2		T3	
cluster	**A**	**B**	**C**	**B**	**C**	**B**	**C**	**B**	**C**
				ethene π complex					
C1–C2	1.322	1.322	1.322	1.322	1.322	1.322	1.322	1.322	1.322
	1.338	*1.337*	*1.338*	*1.337*	*1.337*	1.337	*1.337*	*1.337*	*1.337*
C1–H	2.500	2.503	2.484	2.503	2.497	2.508	2.478	2.488	2.528
	2.253	*2.275*	*2.267*	*2.275*	*2.267*	*2.290*	*2.248*	*2.254*	*2.279*
C2–H	2.500	2.574	2.526	2.574	2.568	2.528	2.497	2.471	2.525
	2.260	*2.344*	*2.314*	*2.344*	*2.330*	*2.311*	*2.280*	*2.245*	*2.273*
Si–O1	1.695	1.696	1.677	1.696	1.675	1.700	1.679	1.709	1.685
	1.708	*1.704*	*1.686*	*1.704*	*1.684*	*1.707*	*1.687*	*1.717*	*1.692*
O1–H	0.959	0.961	0.962	0.961	0.962	0.961	0.963	0.961	0.962
	0.987	*0.987*	*0.990*	*0.987*	*0.989*	*0.987*	*0.991*	*0.989*	*0.991*
Si-O2-Al	156.0	149.0	150.7	143.9	142.3	146.0	149.0	148.0	150.5
	146.6	*146.9*	*150.3*	*140.4*	*137.8*	*143.5*	*148.7*	*145.5*	*150.5*
				ethoxide					
C1–C2	1.514	1.513	1.514	1.514	1.513	1.514	1.511	1.514	1.512
	1.517	*1.513*	*1.514*	*1.515*	*1.514*	*1.511*	*1.512*	*1.514*	*1.512*
C2–O2	1.451	1.482	1.488	1.486	1.490	1.493	1.495	1.489	1.498
	1.471	*1.503*	*1.511*	*1.508*	*1.513*	*1.510*	*1.521*	*1.511*	*1.521*
Si–O1	1.612	1.615	1.588	1.606	1.579	1.615	1.583	1.618	1.584
	1.632	*1.635*	*1.607*	*1.624*	*1.597*	*1.633*	*1.596*	*1.636*	*1.599*
C-O2-Al	120.2	107.7	107.4	108.9	106.7	107.8	106.5	108.8	108.0
	120.3	*108.6*	*108.6*	*109.8*	*107.6*	*108.5*	*106.7*	*109.5*	*108.0*
Si-O2-Al	119.9	136.5	134.3	135.7	135.0	137.0	135.4	136.6	134.6
	120.0	*136.2*	*133.6*	*134.7*	*133.2*	*136.5*	*135.5*	*135.9*	*134.5>*
				transition state					
O1–H	1.453	1.509	1.542	1.549	1.586	1.564	1.633	1.533	1.562
	1.338	*1.419*	*1.488*	*1.433*	*1.492*	*1.465*	*1.547*	*1.439*	*1.528*
C1–H	1.243	1.232	1.247	1.218	1.232	1.211	1.212	1.222	1.244
	1.292	*1.255*	*1.230*	*1.245*	*1.231*	*1.226*	*1.198*	*1.240*	*1.210*
C1–C2	1.385	1.385	1.372	1.386	1.374	1.387	1.377	1.387	1.371
	1.397	*1.401*	*1.400*	*1.402*	*1.400*	*1.404*	*1.405*	*1.403*	*1.403*
C2–O2	2.388	2.510	2.691	2.591	2.792	2.578	2.703	2.532	2.717
	2.153	*2.221*	*2.335*	*2.239*	*2.361*	*2.242*	*2.324*	*2.229*	*2.333*
Si–O1	1.639	1.644	1.609	1.639	1.603	1.645	1.604	1.652	1.612
	1.669	*1.665*	*1.631*	*1.658*	*1.626*	*1.663*	*1.622*	*1.673*	*1.629*
C2-O2-Al	118.0	98.7	96.0	94.5	89.3	96.6	100.3	99.3	96.0
	122.3	*104.2*	*101.0*	*103.4*	*98.9*	*102.8*	*102.4*	*104.3*	*102.0*
Si-O2-Al	129.2	146.5	149.4	145.3	144.9	148.6	150.7	147.9	151.7
	126.2	*142.4*	*143.7*	*140.2*	*139.0*	*143.3*	*145.8*	*143.3*	*146.0*

increases to almost 10°. When the degree of geometry relaxation increases, that is, when cluster **C** instead of cluster **B** is used in the optimizations, the calculated Si–O1 bond length shortens from 1.70 to 1.68 Å and that of Si–O2 shortens from 1.61–1.63 to 1.59–1.60 Å, this being the only observed variation. With respect to the geometry of the particular site considered, the only noticeable difference corresponds to the optimized value of the O1-Al-O2 angle at the T1b site (101.8°), which is between 5° and 10° greater than in any other site.

When the geometry of the ethoxide is analyzed, a big difference is observed between the values obtained with cluster **A** and those obtained with a cluster that represents a particular site in zeolite theta-1. The carbon atom is more covalently bound to the framework oxygen when cluster **A** is used, as reflected in the calculated C2–O2 bond lengths (1.45–1.47 Å in cluster **A** and 1.49–1.51 Å in the others). Notably, the values of the C-O2-Al and Si-O2-Al angles obtained with cluster **A** are 120°, and the C2, O2, Si, and Al atoms are in the same plane. When the cluster used is restricted so as to represent a particular active site in a real zeolite, the geometric changes necessary for the O atom to adopt this conformation become impossible. Thus, for example, the C-O2-Al angles obtained with either cluster **B** or **C** are always between 107 and 110°, while the calculated Si-O2-Al angles are never smaller than 133°. As regards the cluster size, the most relevant differences observed when going from cluster **B** to **C** are related to Si–O1 and C2–O2 bond lengths. The former decrease from 1.61–1.63 Å in cluster **B** to 1.58–1.60 Å in cluster **C**, while the latter increase slightly suggesting a certain degree of correlation between the alkoxide C–O bond strength and cluster size.

The ethene protonation reaction occurs through a concerted mechanism that involves the transition state depicted in Figure 3b. At the same time as when the hydrogen atom of the bridging hydroxy group protonates one of the carbon atoms of ethene (C1), the positive charge that appears on C2 interacts with one of the neighboring basic oxygen atoms of the zeolite to result in the formation of the covalent ethoxide complex. The geometry of the transition state optimized by means of different models and theoretical methods is given in Table 3. In all cases, the proton that is being transferred from the zeolite to the ethene molecule is closer to the carbon than to the oxygen atom. The calculated C1–H bond lengths are ≈1.2 Å in all cases, while the O1–H bond lengths calculated with clusters **B** and **C** are about 0.1 and 0.15 Å, respectively, longer than those obtained with cluster **A**. The same tendency is observed for the C2–O2 bond lengths: the values obtained with cluster **A** are ≈0.1 and ≈0.3 Å shorter than those calculated with clusters **B** and **C**, respectively. This indicates that, as the cluster becomes more similar to the real zeolite, the organic fragment in the transition state it located further from the catalyst wall. It has also been observed that, while on cluster **A** the C1, C2, H, O1, O2, and Al atoms are more or less coplanar, when clusters **B** and **C** are used the organic

fragment tends to move away from this position and to be located out of the plane of the 10-T ring. It is also to be noted that the differences previously mentioned between the geometry of the ethoxide complex obtained with cluster **A** and those provided by the clusters that represent active sites in zeolite theta-1 begin to be observed in the transition state. Thus, for example, the C-O2-Al and Si-O2-Al angles calculated with cluster **A** are close to 120° and 130°, respectively, while the values obtained with clusters **B** and **C** are between 90° and 105° in the first case and between 140° and 150° in the second one.

Action and reaction energies: The reaction energies ΔE of the ethene protonation reaction (Table 4) have been calculated as the total energy difference between the ethoxide and the ethene π complex, and therefore negative values indicate that the covalent ethoxide is more stable than adsorbed ethene. The first remarkable result concerning the calculated values of ΔE is the great difference existing between the values obtained with cluster **A** and those obtained with a cluster that represents a particular active site in theta-1 zeolite. It can be seen that when cluster **A** is used, the covalent ethoxide is more stable by 11.7 kcal mol^{-1} at the HF level and 13.8 kcal mol^{-1} at the B3LYP level than the adsorbed ethene. However, when the geometry of the cluster is restricted to simulate a particular active site, the ethoxide is greatly destabilized in relation to the ethene π complex. Thus, for example, the HF calculated ΔE values are between -1.5 and $+6.3$ kcal mol^{-1}, depending on the considered site and on the cluster used. DFT calculations seem to slightly increase the relative stability of the ethoxide, and the calculated ΔE values are between -5.5 and $+2.2$ kcal mol^{-1}. The most negative ΔE values are obtained when the reaction occurs on the T1 site, while on T2 and T3 sites the ethoxide is considerably less stable than the adsorbed ethene. With respect to the influence of the zeolite flexibility or the cluster size on the calculated reaction energies, no clear tendencies are observed, while periodic calculations yield higher reaction energies on all sites.

Table 4. Reaction energies [kcal mol^{-1}] calculated at the HF and B3LYP levels.[a]

	HF				B3LYP			
	T1a	T1b	T2	T3	T1a	T1b	T2	T3
B	−1.53	0.71	5.49	2.14	−5.49	−3.67	−0.48	−2.40
C	−0.64	0.28	4.85	4.79	−4.77	−3.93	1.18	0.27
D	−0.64	0.16	4.66	6.31	−4.92	−3.88	0.73	2.15
periodic	3.86	2.59	7.25	11.68				

[a] The values calculated with cluster **A** are −11.68 and −13.75 kcal mol^{-1} at the HF and B3LYP levels, respectively.

Some of these energetic differences can be easily related to optimized geometries of the ethoxide as discussed above. The ethoxide complex is more strongly bonded to the framework oxygen when cluster **A** is used, as reflected in the shorter calculated C2−O2 bond length (1.45 and 1.47 Å at the HF and B3LYP levels, respectively). When the reaction occurs on the T1 site, the calculated C2−O2 bond lengths are ≈1.48 – 1.49 Å at the HF level and − 50 – 1.51 Å at the B3LYP level, while on T2 and T3 sites the obtained values are slightly longer, 1.49 – 1.50 Å at the HF level and 1.51 – 1.52 Å at the B3LYP level. Therefore, the increase in the C2−O2 bond length reflects a weakening of the covalent bond and therefore a destabilization of the ethoxide.

The additional increase in the reaction energy provided by the periodic calculations is mainly attributed to the fact that the geometries were not optimized at the periodic level but rather with cluster **C**. To illustrate this, let us consider Figure 4 which shows the HF-optimized structures of the four ethoxide complexes studied adsorbed on cluster **D**. While on T1b and T2 sites the organic fragment is situated inside the cluster and is therefore completely surrounded by oxygen and silicon atoms, on T1a and especially on T3, most of the organic fragment is situated near the edge of the cluster. It is then to be expected that the most important differences between cluster **D** and periodic results will be observed on T1a and on T3, as has been indeed found. Nevertheless, even on T1b and T2 there is a difference of 2.5 kcal mol^{-1} between the cluster **D** and the periodic calculated reaction energies which can not be attributed to this representation. To explain this observation, the Mulliken charge distribution in the cluster and in the periodic systems has been analyzed in depth. The oxygen atoms in the periodic system are ≈0.01 e more negatively charged than in cluster **D**, both in the case of the adsorbed ethene and in the case of the ethoxide. Notably, although the

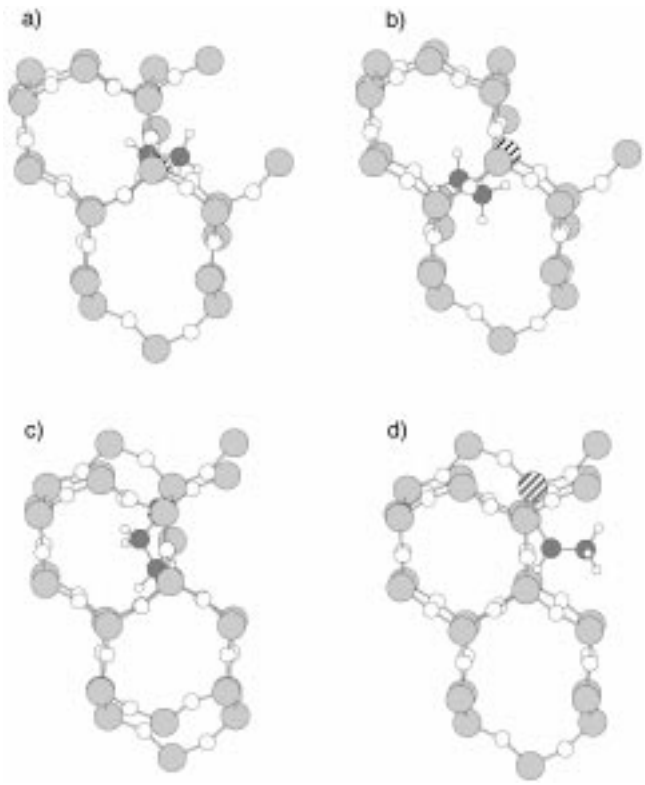

Figure 4. HF/6-31G*-optimized structures of the ethoxide complex adsorbed on a) T1a, b) T1b, c) T2, and d) T3 sites. Cluster **D** is shown.

0947-6539/01/0706-1300 $ 17.50+.50/0 *Chem. Eur. J.* **2001**, *7*, No. 6

differences in population are small, they are relevant because the systems compared have been calculated at the same geometry and level of theory. Therefore, changes in the population analysis can only be related to differences between the character of the electronic structure in the large (and quite "realistic") cluster **D** and in the crystalline catalyst. The slightly larger electron population on the O atoms provided by the periodic calculations reflects an enhancement of the system ionicity that causes a loss of covalent character in the C2–O2 bond. Following the trend observed when increasing the cluster size, it is to be expected that further geometry relaxation in the periodic model would result in an increase of the C2–O2 bond length and a lowering of the reaction energy. Also, we have tested that in both the cluster **D** and the periodic models, the distances between hydrogens atoms of the ethoxy group and zeolitic O atoms are always larger than 2.2 Å. This fact discards the possibility that the alkoxy groups be additionally stabilized in the periodic model because of hydrogen bond interactions.

The activation energies summarized in Table 5 have been calculated as the total energy difference between the transition state and the reactant, which is the ethene π complex.

Table 5. Activation energies [kcal mol^{-1}] calculated at the HF and B3LYP levels.[a]

	HF				B3LYP			
	T1a	T1b	T2	T3	T1a	T1b	T2	T3
B	41.89	42.78	44.37	43.88	25.01	26.38	28.09	27.14
C	38.41	39.09	42.59	40.37	24.63	25.54	29.11	27.28
D	35.52	36.14	38.84	39.61	23.18	23.86	27.64	27.92
periodic	36.24	36.03	38.49	36.21				

[a] The values calculated with cluster **A** are 42.55 and 25.67 kcal mol^{-1} at the HF and B3LYP levels, respectively.

The most important factor influencing the activation energy is the methodology used. When electron correlation effects are included by means of DFT, the activation energies are lowered between 11 and 17 kcal mol^{-1}. The results obtained with cluster **A** are not too different from those obtained with cluster **B**; however, when each site is considered separately a dependence between the calculated activation energies and the cluster size is found at the HF level. Thus, at the HF level, when cluster **D** instead of cluster **C** is used, the activation barrier is 1–4 kcal mol^{-1} lower, and a similar stabilization occurs when cluster **C** instead of cluster **B** is used. An explanation for this behavior is that while the reactant and the reaction product are neutral species, the transition state is highly ionic, and therefore electrostatic effects have a greater influence on its energy. Although the cluster approach is not well suited to treat these effects, it is obvious that as the cluster size increases, the model is more similar to a real zeolite and electrostatic effects are somewhat included. In fact, the activation energies calculated with cluster **D** are very similar to those obtained with the periodic approach, which introduces all short- and long-range electrostatic effects.

Another point of view can be obtained by studying the electronic structure of the transition state. The Mulliken population analysis indicates that on all sites, as the size of the cluster increases, the net atomic charge on the H atom that is being transferred decreases, while no clear tendencies are found for either the charges on the carbon atoms or for the global charge on the organic fragment. The charge decrease on the H1 atom when passing from cluster **C** to the periodic model is ≈0.01 e in all cases.

Figure 5 shows the difference map between the electronic density of periodic and cluster **C** transition states on the T2 site. Electron density has been calculated on the plane parallel

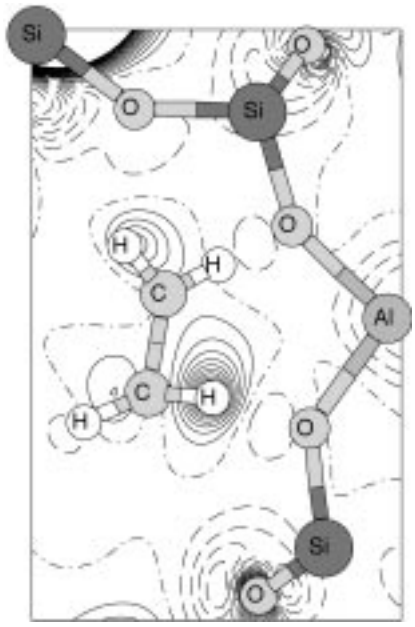

Figure 5. Electron density difference map between periodic and cluster **C** models of the transition state on T2 site. Isodensity lines are at each 2×10^{-4} |e|.

to *xy* that contains the H1 atom. Differences between both models are, in general, small in the region where the reaction occurs. Nevertheless, in straight correlation with the Mulliken population analysis, electron density on H1 is larger in the periodic model than in cluster **C**. On the other hand, the electron density along the lines connecting atoms H1–O1 and C2–O2 is slightly larger in cluster **C** than in the periodic model. This is to be associated with a more ionic character of the transition state in the periodic model. The enhancement of ionicity in periodic calculations has been previously discussed in relation to the stability of the ethoxide-zeolite complex. The main difference is that, while in that case the increase in ionicity results in a destabilization of the covalent C2–O2 bond, in this case, because of the charge separation existing in the transition state, the overall effect is to stabilize the ion–pair complex.

At the B3LYP level, the stabilization of the transition state caused by the increase of the cluster size is less important, and varies between 0 and 2 kcal mol^{-1}. This is in agreement with the previous explanation. According to the Mulliken population analysis, the positive charge on the $C_2H_5^+$ fragment of the transition state is +0.8 e at the HF level and only +0.5 e at the B3LYP level, independent of the cluster used. This means

that the ionic character of the transition state is more marked at the HF level and therefore the stabilization of this structure as a result of electrostatic effects should be more important at this level, as has been indeed found.

Conclusions

The protonation of ethene by three different acid sites of theta-1 zeolite to give covalent ethoxide intermediates has been theoretically investigated by means of cluster and periodic calculations, and the influence of the methodology used, of the cluster size and degree of geometry relaxation, and of the global effects caused by the whole crystal have been analyzed.

It has been found, in agreement with previous work,[28] that the stability of the ethoxide complex is very sensitive to the local geometry of the active site, with the calculated reaction energies covering a range of up to 9 kcal mol^{-1}. The main reason is that the structural changes necessary to accommodate the covalent ethoxide become more difficult when the geometry of the system is restricted to represent a particular site in a particular zeolite and, as a consequence, the ethoxide is greatly destabilized with respect to adsorbed ethene. It has also been observed that long-range effects included in periodic calculations tend to increase the ionicity of the systems, to produce an additional destabilization of the covalent ethoxides. In fact, in many cases, the reaction energy ΔE is positive which indicates that the ethoxide is less stable than the initial reactant. From a chemical point of view, this means that covalent alkoxides can be reactive intermediates in many zeolite-catalyzed reactions since they are not as stable as earlier cluster calculations suggested and therefore the real activation energies involved will not be so high. From a methodological point of view, it can be concluded that when the cluster approach is used, complete optimization of all the geometric parameters of the system is not recommendable since it will often yield unrealistic energies.

The local arrangement of the active site and the degree of geometry optimization have little influence on the activation energies, which are mainly affected by the methodology used and by electrostatic effects. Thus, inclusion of electron correlation effects by means of DFT lowers the calculated activation barriers by more than 10 kcal mol^{-1}. With respect to the electrostatic effects, it has been found that as the cluster size increases and more oxygen atoms are included in the system, the transition state becomes more stable in relation to ethene and ethoxide. The reason is that while the reactant and the product are neutral species, the transition state is highly ionic and therefore it is stabilized by the negative potential created by the oxygen atoms of the catalyst. The lowering of the activation energy at the HF level ($\approx$6 kcalmol^{-1}) is more important than at the DFT level ($\approx$2 kcalmol^{-1}) because the ionic character of the transition state, represented by the net positive charge on the $C_2H_5^+$ fragment, is more marked at the HF level.[29]

In synthesis, as the model becomes more realistic, changes in both the reaction and the activation energies are observed, although the causes are different in each case. Reaction energies are mainly affected by structural relaxation. In addition, there is a weakening of the covalent C–O bond in the ethoxide which is related to a slight increase of the ionicity as the system size approaches the periodic limit of the model. On the other hand, activation energies are not so dependent on geometry restrictions but, because of the ionic character of the transition state, they are mainly influenced by electrostatic effects that rapidly converge with cluster size. It is to be stressed that this stabilization mainly involves the O atoms of the channel wall that are within the closest region around the organic fragment, no matter whether or not long-range electrostatic effects are included in the calculation.

Acknowledgements

The authors thank the Departament de Química Física of the University of Valencia for computing facilities. They thank C.I.C.Y.T. (Project MAT 97-1016-C02-01) and Conselleria de Cultura, Educació i Ciència de la Generalitat Valenciana for financial support. M.B. thanks the I.T.Q. for a post-doctoral grant.

[1] A. Corma, *Chem. Rev.* **1995**, *95*, 559.
[2] B. W. Wojcechowski, A. Corma, *Catalytic Cracking: Catalysts, Chemistry and Kinetics*, Dekker, New York, **1986**.
[3] G. A. Olah, G. K. S. Prakash, J. Sommer, *Superacids*, Wiley-Interscience, New York, **1995**.
[4] P. A. Jacobs, *Carboniogenic Activity of Zeolites*, Elsevier, New York, **1977**.
[5] C. M. Zicovich-Wilson, P. Viruela, A. Corma, *J. Phys. Chem.* **1995**, *99*, 13224–13231.
[6] F. Haase, J. Sauer, *J. Am. Chem. Soc.* **1995**, *117*, 3780.
[7] P. Viruela, C. M. Zicovich, A. Corma, *J. Phys. Chem.* **1993**, *97*, 13713.
[8] C. J. A. Mota, P. M. Esteves, M. B. de Amorim, *J. Phys. Chem.* **1996**, *100*, 12418.
[9] G. J. Kramer, R. A. van Santen, *J. Am. Chem. Soc.* **1995**, *117*, 1766.
[10] S. R. Blaszkowski, A. P. J. Jansen, M. A. C. Nascimento, R. A. van-Santen, *J. Phys. Chem.* **1994**, *98*, 12938.
[11] S. R. Blaszkowski, M. A. C. Nascimento, R. A. van Santen, *J. Phys. Chem.* **1996**, *100*, 3463.
[12] M. V. Frash, V. B. Kazansky, A. M. Rigby, R. A. van Santen, *J. Phys. Chem. B* **1998**, *102*, 2232.
[13] S. J. Collins, P. J. O'Malley, *J. Catal.* **1995**, *153*, 94.
[14] V. B. Kazansky, M. V. Frash, R. A. van Santen, *Appl. Catal. A: General* **1996**, *146*, 225.
[15] M. Boronat, P. Viruela, A. Corma, *J. Phys. Chem. A* **1998**, *102*, 982.
[16] M. V. Frash, V. B. Kazansky, A. M. Rigby, R. A. van Santen, *J. Phys. Chem. B* **1997**, *101*, 5346.
[17] M. Boronat, P. Viruela, A. Corma, *J. Phys. Chem. A* **1998**, *102*, 9863.
[18] V. B. Kazansky, M. V. Frash, R. A. van Santen, *Stud. Surf.Sci. Catal.* **1997**, *105*, 2283.
[19] M. Boronat, P. Viruela, A. Corma, *Phys. Chem. Chem. Phys.*, in press.
[20] C. Pisani, R. Dovesi, C. Roetti, *Hartree-Fock ab initio Treatment of Crystalline Solids in Lecture Notes in Chemistry Series*, *Vol. 48*, Springer, Berlin, **1988**.
[21] C. M. Zicovich-Wilson, R. Dovesi, A. Corma, *J. Phys. Chem.* **1999**, *103*, 988–994.
[22] P. Ugliengo, B. Civalleri, C. M. Zicovich-Wilson, R. Dovesi, *Chem. Phys. Lett.* **2000**, *318*, 247–255.
[23] V. B. Kazansky, *Acc. Chem. Res.* **1991**, *24*, 379.
[24] M. T. Aronson, R. J. Gorte, W. E. Farneth, D. White, *J. Am. Chem. Soc.* **1989**, *111*, 840.
[25] J. F. Haw, B. R. Richardson, I. S. Oshiro, N. D. Lazo, J. A. Speed, *J. Am. Chem. Soc.* **1989**, *111*, 2052.
[26] N. D. Lazo, B. R. Richardson, P. D. Schettler, J. L. White, E. J. Munson, J. F. Haw, *J. Phys. Chem.* **1991**, *95*, 9420.

  0947-6539/01/0706-1302 $ 17.50+.50/0

[27] V. G. Malkin, V. V. Chesnokov, E. A. Paukshtis, G. M. Zhidomirov, *J. Am. Chem. Soc.* **1990**, *112*, 666.
[28] P. E. Sinclair, A. de Vries, P. Sherwood, C. R. A. Catlow, R. A. van Santen, *J. Chem. Soc. Faraday Trans.* **1998**, *94*, 3401–3408.
[29] M. Boronat, C. M. Zicovich-Wilson, A. Corma, P. Viruela, *Phys. Chem. Chem. Phys.* **1999**, *1*, 537–543.
[30] S. A. Zygmunt, L. A. Curtiss, P. Zapol, L. E. Iton, *J. Phys. Chem. B* **2000**, *104*, 1944–1949.
[31] S. A. I. Barri, G. W. Smith, D. White, D. Young, *Nature* **1984**, *312*, 533–534.
[32] R. M. Highcock, G. W. Smith, D. Wood, *Acta Crystallogr.* Sect. *C* **1985**, *41*, 1391–1394.
[33] GULP (The General Utility Lattice Program) written and developed by J. D. Gale, Royal Institution/Imperial College, UK, **1992–1994**.
[34] K. P. Schröder, J. Sauer, *J. Phys. Chem*. **1996**, *100*, 11043.
[35] a) A. D. Becke, *J. Chem. Phys.* **1993**, *98*, 5648. b) C. Lee, W. Yang, R. G. Parr, *Phys. Rev. B* **1988**, *37*, 785.
[36] P. C. Hariharan, J. A. Pople, *Chem. Phys. Lett.* **1972**, *16*, 217.
[37] H. B. Schlegel, *J. Comput. Chem.* **1982**, *3*, 214.
[38] M. J. Frisch, G. W. Trucks, H. B. Schlegel, P. M. W. Gill, B. G. Johnson, M. A. Robb, J. R. Cheeseman, T. Keith, G. A. Petersson, J. A. Montgomery, K. Raghavachari, M. A. Al-Laham, V. G. Zakrzewski, J. V. Ortiz, J. B. Foresman, J. Cioslowski, B. B. Stefanov, A. Nanayakkara, M. Challacombe, C. Y. Peng, P. Y. Ayala, W. Chen, M. W. Wong, J. L. Andres, E. S. Replogle, R. Gomperts, R. L. Martin, D. J. Fox, J. S. Binkley, D. J. DeFrees, J. Baker, J. P. Stewart, M. Head-Gordon, C. Gonzalez, J. A. Pople, Gaussian 94, Revision B.1, Gaussian: Pittsburgh, PA, 1995.
[39] P. Ugliengo, B. Civalleri, R. Dovesi, C. M. Zicovich-Wilson, *Phys. Chem. Chem. Phys.* **1999**, *1*, 545.
[40] V. R. Saunders, R. Dovesi, C. Roetti, M. Causà, N. M. Harrison, R. Orlando, C. M. Zicovich-Wilson, C. M. *CRYSTAL 98 User's Manual*, Università di Torino, Turin (Italy), **1999**.

Received: July 5, 2000
Revised: November 28, 2000 [F2586]